Journal of Electroceramics 2:4, 283–293, 1998

Giant Magnetoresistance and Its Sensor Applications

K. INOMATA
Advanced Research Laboratory, Toshiba Corporation, Kawasaki 210, Japan

Submitted September 10, 1997; Revised June 18, 1998; Accepted June 24, 1998

Abstract. Current status is addressed for spin polarized transport such as spin-dependent scattering and spin-dependent tunneling in artificial structured magnetic thin films. The main points discussed include the physical origin of the giant magnetoresistance (GMR) and various GMR materials. The applications of the GMR to magnetic sensors such as read heads for ultra high density magnetic recording are also discussed.

Keywords: giant magnetoresistance, tunnel magnetoresistance, HDD, heads

1. Introduction

Magnetoresistance is the change in electrical resistance of a material in response to a magnetic field. All metals have an inherent, albeit small, magnetoresistance (MR) owing to the Lorenz force that a magnetic field exerts on moving electrons. However, metallic alloys containing magnetic atoms can have an enhanced MR because the scattering that produces the electrical resistance is controlled by a magnetic field. Today, for example, permalloy (an alloy of nickel and iron) is used as a magnetoresistive sensor in reading heads in magnetic hard disk drives in computers. In 1988 a more dramatic MR effect, which is called giant magnetoresistance (GMR) effect, was discovered [1] in a multilayer structured material that makes this structure a candidate for reading heads in the next generation of information storage systems. After the discovery in the magnetic multilayer the GMR effect was observed in many magnetic multilayers including Co/Cu [2,3] and NiFe/Cu/Co/Cu [4] and in granular alloy films [5,6]. The physical origin of the GMR has been revealed to be spin-dependent scattering of conduction electrons at the interfaces between ferromagnetic and nonmagnetic metals. The spin-valve structures exhibiting low-field GMR were developed [7] and have been studied for micro spin-electronic devices such as GMR read heads for ultra high density magnetic recording [8,9] and magnetic random access memories (MRAM) [10–12].

The GMR has also stimulated the spin-dependent tunneling in the ferromagnetic tunnel junctions [13] and in insulating granular films with fine metallic particles embedded in an insulating matrix [14]. The magnetoresistance in the ferromagnetic tunnel junctions (TMR) can exceed the spin-valve GMR [15–18], although there are some subjects to be surmounted from the point of applications. Thus, the study is increasing for TMR as post-spin valve materials.

In this paper the current status is addressed for spin polarized transport such as spin-dependent scattering and spin-dependent tunneling in artificial structured magnetic thin films such as magnetic multilayers, magnetic granular systems and ferromagnetic tunnel junctions. In addition, applications of GMR to magnetic field sensors such as read heads for ultra high density magnetic recording are discussed.

2. Anisotropic Magnetoresistance

Magnetoresistance is usually measured using the 4 point method as shown in Fig. 1(a). The sample has strip shape, and the current (I) is applied along the long axis of the strip in order to obtain the uniform current flow between the voltage terminals. The sample is set to be rotated in a magnet in order that the resistance can be measured in an arbitrary field direction with respect to the current.

Before discussing the GMR the anisotropic

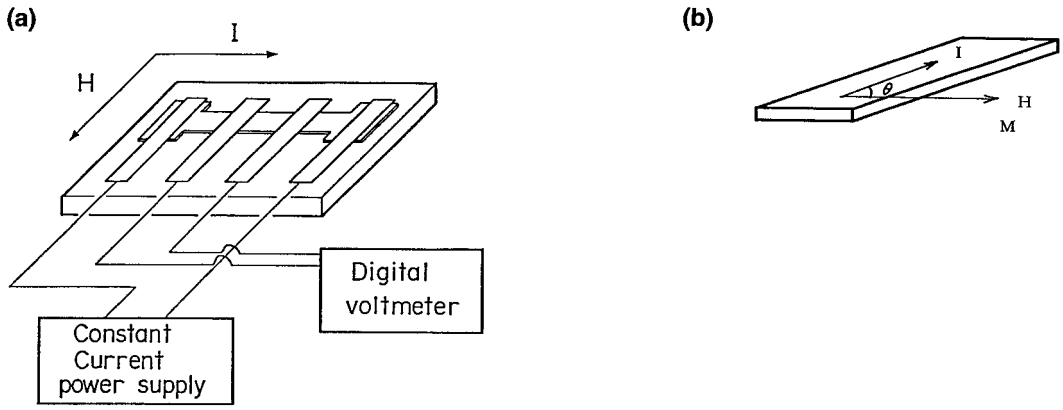

Fig. 1. Measurement method of the magnetoresistance (a) and a relation between current and magnetic field directions.

magnetoresistance (AMR) in ferromagnetic metals is briefly explained. The AMR is associated with the direction of magnetization relative to the current, originated from the spin-orbit interaction. In a thin film where magnetization M makes an angle θ with current I in a film plane as shown in Fig. 1(b) the resistivity $\rho(\theta)$ is given by

$$\rho(\theta) = \rho_0 + \Delta\rho \cos^2\theta \tag{1}$$

When we denote $\rho_{||}$ and $\rho_{\perp}$ as the resistivity for magnetization parallel and perpendicular to the current, respectively, Eq. (1) can be written as

$$\rho(\theta) = \rho_{\perp} \sin^2\theta + \rho_{||} \cos^2\theta \tag{2}$$

where,

$$\Delta\rho = \rho_{||} - \rho_{\perp} \tag{3}$$

The AMR gives positive $\Delta\rho$. The maximum MR ratio, $\Delta\rho/\rho_{av}$ is about 6% at RT for a $Ni_{80}Co_{20}$ alloy, where ρ_{av} is $\rho_{||}/3 + 2\rho_{\perp}/3$. Today, permalloy, a Ni-Fe alloy with MR ratio of about 3% is used in high density magnetic recording read heads, because it has soft magnetic properties.

3. GMR in Metallic Multilayers

3.1. Discovery of the GMR

The GMR was discovered by Baibich et al. in 1988 for Fe/Cr multilayers prepared by the Molecular Beam Epitaxy (MBE) method, which is shown in Fig. 2 (a) [1]. The resistivity normalized by the zero field value in (Fe 30 Å /Cr t Å)$_n$ multilayers drops dramatically with increasing field and saturates at a field that depends on the Cr layer thickness. The MR ratio depends on the Cr layer thickness, and the maximum drop is about 0.45 for (Fe 30 Å/Cr 9 Å)$_{60}$ at 4.2 K. The successive magnetic layers across a non-magnetic layer have an anti ferromagnetic (AF) arrangement at zero field due to the interlayer AF coupling and a ferromagnetic (F) one at a saturation field. If we define the MR ratio by $(R_{AF}\text{-}R_F)/R_F$, where R_{AF} and R_F are the resistance of zero and saturation fields, respectively, the above 0.45 corresponds to the MR ratio of 0.85. This is significantly larger than that of the AMR. The GMR does not depend on applied field directions, contrary to the AMR as shown in Fig. 2(b), in which the field is applied to three directions: along the current direction in the film plane (1), transverse to the current in the film plane (2), perpendicular to the film plane (3). The saturation field is higher for (3) because of the large demagnetization field.

After observation of GMR in Fe/Cr, oscillatory GMR was observed in Fe/Cr as a function of Cr layer thickness as shown in Fig. 3 (a), which was prepared by the sputtering method [2]. The MR oscillation was accompanied by the oscillation of the saturation field as seen in Fig. 3(b). Since the saturation field is proportional to the interlayer coupling, the oscillatory saturation field is ascribed to the oscillatory interlayer coupling. The oscillation period is about 1 nm and longer than that due to the Ruderman-Kittel-Kasuya-Yoshida (RKKY) interaction, which has been observed in diluted magnetic metal alloy systems. Thus, this oscillatory behavior

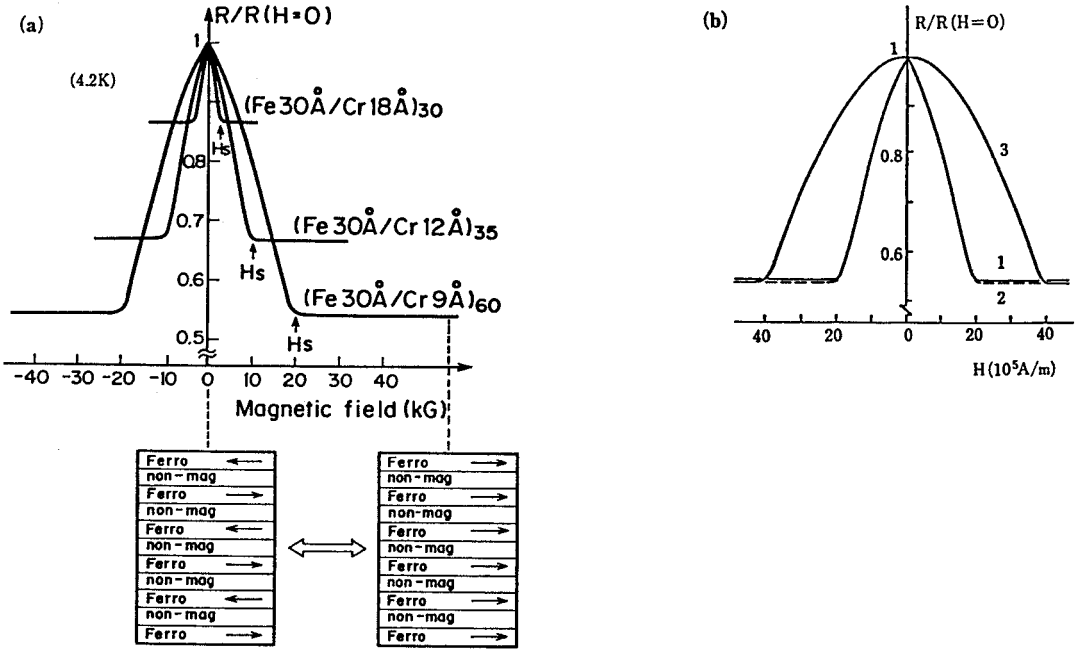

Fig. 2. Giant magnetoresistance in Fe/Cr multilayers. (a) Nomalized MR as a function of field. (b) MR curves for three different field directions [1].

provided a new theme in solid state physics. This subject is not described more because it is outside of the scope of this review.

After the observation of the GMR in Fe/Cr multilayers many multilayer systems consisting of magnetic-nonmagnetic metals have been found to exhibit the GMR effect. Among them Co/Cu [2,3] and Co-Fe/Cu [19] systems exhibit the largest MR at RT, which is shown in Figs. 4 [20] and 5 [21]. The MR exceeds 50% and oscillates with Cu layer thickness as shown in Fig. 4. The oscillation behavior is common to the GMR multilayers, and has been revealed to be attributed to the oscillation of the interlayer exchange coupling between ferromagnetic and antiferromagnetic.

3.2. Mechanism of the GMR

The GMR is attributed to the spin dependent conduction properties of the ferromagnetic metals. In a ferromagnetic metal the electrical current is carried by the spin ↑ (majority) and spin ↓ (minority) electrons in two approximately independent channels. The conductivities of the two channels can be very different, especially when the ferromagnetic metal contains impurities with strongly spin dependent scattering cross sections. In magnetic multilayers electron scattering by imperfect interfaces or by impurities or defects within the magnetic layers can be spin dependent. The schematic of Fig. 6 [22] illustrates the mechanism of the GMR in the simple limit where electrons have a mean free path (MFP) much larger than the layer thicknesses and can feel the relative orientation of the magnetization in successive layers. The electron trajectories between two scatterings are represented by straight lines and the scatterings by abrupt changes in direction. The small arrows $\rightarrow$ and $\leftarrow$ are for electron spins. The large arrows represent the majority spin direction in the magnetic layers. In the F configuration in Fig. 6b, the $\rightarrow$ spin electrons are weakly scattered everywhere, which gives a short circuit effect and leads to small resistivity. In the AF configuration in Fig. 6a, each spin direction is scattered in every second magnetic layer, there is no short circuit effect and the resistivity is higher. When the thickness of the non-magnetic layers becomes larger than the MFP (~ 10 nm), the coupling between successive magnetic layers disappears and the GMR vanishes. An additional reason for the decrease of the GMR at increasing thickness

comes from the importance of interface spin dependent scattering: as the thickness increases, the interface density decreases, which also contributes to the decrease of the resistivity change $\Delta\rho$.

3.3. GMR Multilayer Systems

The GMR for various multilayer systems is shown as a function of the electron number of the magnetic layer in Fig. 5, in which Cu is used as a non-magnetic layer [21]. The MR ratio exhibits a maximum for Co or a Co-rich Co-Fe alloy [19] as a ferromagnetic layer. This maximum depends on investigators because the GMR is influenced by interface structures. The dashed line is the calculated result based on the spin dependent scattering at the interface using the bulk band structure [23]. The calculated result agrees with the experiments qualitatively, but not quantitatively.

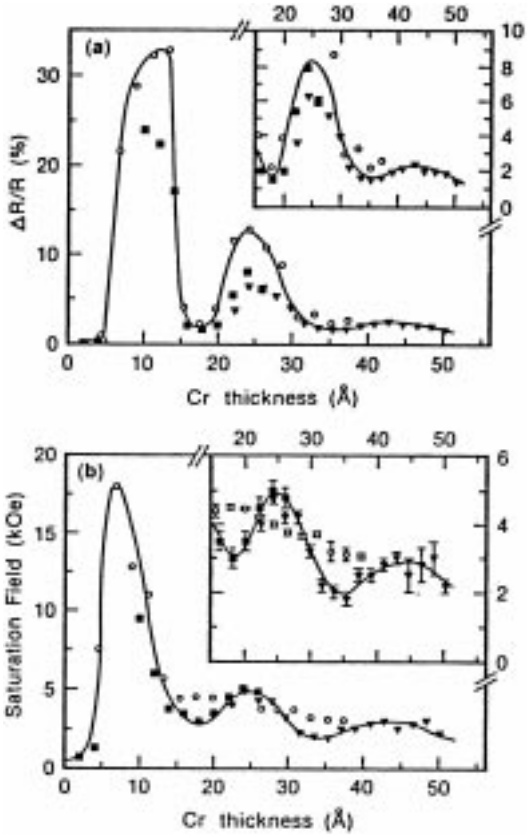

Fig. 3. (a) Saturation magnetoresistance (4.5 K) and (b) saturation field (4.5 K) vs. Cr layer thickness [2].

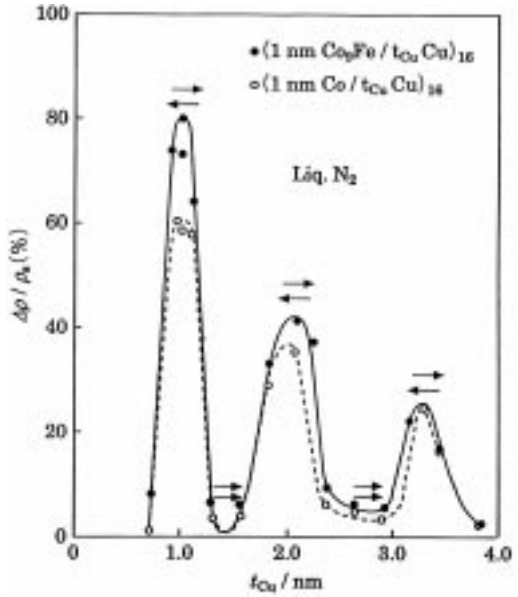

Fig. 4. Magnetoresistance ratio at liq.N_2 temperature for Co/Cu and Co_9Fe/Cu multilayers as a function of Cu layer thickness [20].

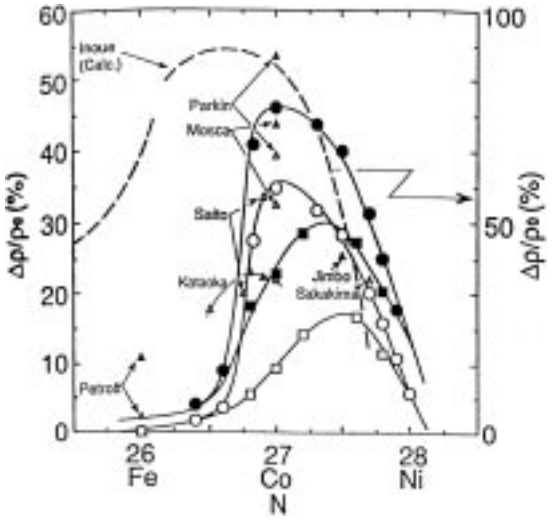

Fig. 5. Variation of MR ratio as a function of electron numbers of the magnetic layer. The solid line is a guide for the eyes and dashed line is calculated result [21].

The microscopic mechanism of the spin dependent scattering by interface is still not very clear.

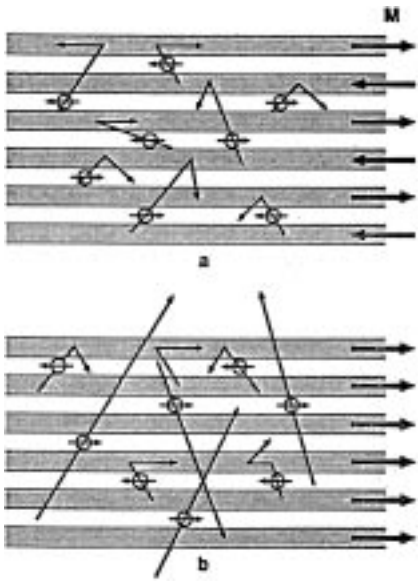

Fig. 6. Schematic of conduction in multilayer magnetic film array, showing how different spin scattering produces a different resistance for parallel (a) and antiparallel (b) film magnetizations [22].

3.4. Spin-Valves

Antiferromagnetic coupling was initially thought to be tied to GMR. Although it is true that in layered structures with large MR, there is a strong AF coupling, the converse is not true, it is not necessary to have this coupling to produce GMR. All that is necessary is that the layers are not ferromagnetically aligned. The saturation field is large in the AF-coupled multilayers, thus the field sensitivity of the GMR is not high. This leads to the difficulty of strongly coupled multilayers to be applied for the magnetic field sensors such as magnetic read heads in hard disk drives (HDD). The spin-valve structure has been developed to overcome the difficulty [7]. The spin-valve structure essentially consists of four layers made of ferromagnet/nonmagnet/ferromagnet/antiferromagnet with a week interlayer coupling between the ferromagnets due to the thicker nonmagnetic layer. The ferromagnetic spins in contact with an antiferromagnetic layer are pinned by a unidirectional exchange anisotropy field. The other ferromagnetic layer spins are freely oriented by an external field, which leads to the high field sensitivity. Thus, the two ferromagnetic layers are named as pinned and free layers for the former and the latter, respectively. The MR curve for a spin-valve is shown schematically in Fig. 7, in which a field was applied along an uniaxial exchange anisotropy. In the low field range the free layer spins only are oriented by an external field, while the pinned layer spins are oriented in the higher field range.

The MR ratio is shown in Fig. 8 for NiFe/Cu and Co_9Fe/Cu spin-valves as a function of the magnetic layer thickness, compared with the AMR for a NiFe alloy film [24]. The MR ratio for the Co_9Fe/Cu spin-valve is higher than that for the NiFe/Cu spin-valve, and increases up to 13% by annealing at 250°C. This means that the Co_9Fe/Cu spin-valve has high thermal stability, which is important for the sensor applications. The antiferromagnetic layer is very important in spin-valves, because it must pin the neighboring ferromagnetic layer spins. The large exchange coupling field and the high blocking temperature (a temperature over which the pinning field disappears) are required as well as corrosion resistance for the antiferromagnets. Many antiferromagnetic materials have been studied including disordered fcc Mn alloys such as FeMn and IrMn, ordered fct alloys such as NiMn and PtMn and oxides such as NiO and α-Fe_2O_3, which are summarized in Table 1. Antiferromagnets meeting all the above requirements have not been found, although GMR heads using the spin-valves have been developed as described in the following.

4. Other GMR Materials

4.1. Granular Alloys

Considering that the GMR originates from the spin-dependent scattering at the interfaces we can expect the GMR effect for other systems in addition to metallic multilayers. The GMR has been observed in metallic granular systems in which nano-sized magnetic metal particles are embedded in a non-magnetic metal matrix, as shown schematically in Fig. 9 [5,6]. The spin-dependent scattering occurs at the interfaces between the nano-sized particles and the matrix. The particle size is smaller than 5 nm, and the distance between the particles is below 10 nm, lower than the mean free path in the granular GMR materials. The maximum GMR has been observed to be about 30% at RT for a Co-Ag system. This is

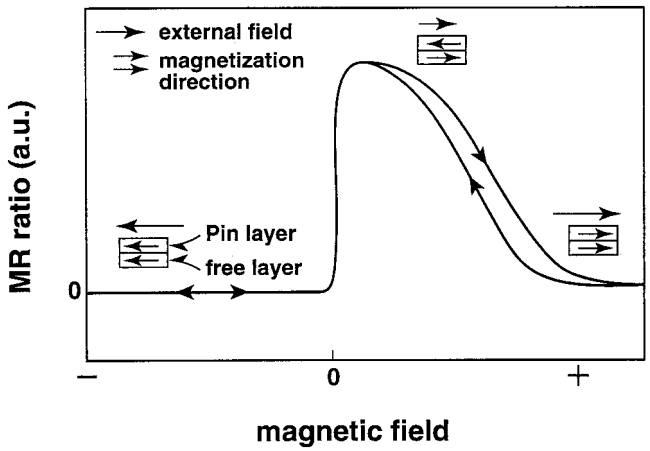

Fig. 7. Schematic MR ratio as a function of magnetic field for a spin valve.

significantly larger than that of the spin-valves. The saturation field, however, is over 1 T because of the superparamagnetic nature of the nano-sized particles. This prevents the granular GMR materials to be applied for the magnetic field sensors.

4.2. *Ferromagnetic Tunnel Junctions*

The tunnel magnetoresistance (TMR) in ferromagnetic tunnel junctions consisting of ferromagnetic-insulator-ferromagnetic (FM-I-FM) has been already observed 20 years ago [13]. After the discovery of the GMR in metallic multilayers the TMR has been re-examined. The basic principle of the TMR is spin-dependent tunneling, which is ascribed to the spin-dependent density of states at the Fermi level of ferromagnets, assuming that spin is conserved in tunneling and tunneling current is dependent on the density of states of the two electrodes. According to the models of Julliere [13] and Maekawa et al. [25] the conductance G is given by

$$G = \sum_{\sigma} |T|^2 D_{1_\sigma}(E_F) D_{2_\sigma}(E_F + eV) \tag{4}$$

where

$$|T|^2 \propto \exp(-2s\chi), \chi = [8\pi m(\phi - E_F)/h^2]^{1/2} \tag{5}$$

and $D(E_F)$ and σ are the density of state at the Fermi level and the spin, respectively. ϕ and s are the

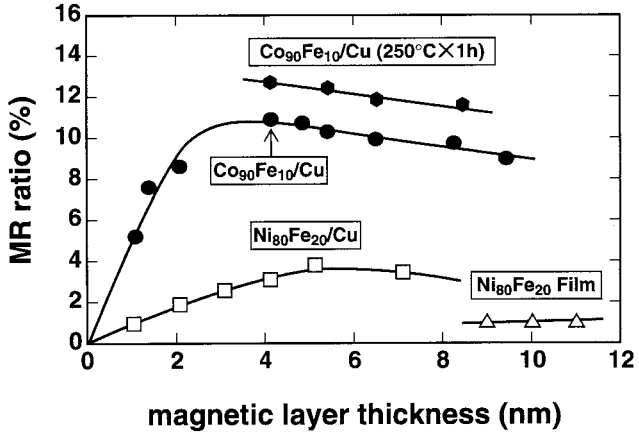

Fig. 8. MR ratio for Co_9Fe/Cu and NiFe/Cu spin valves and NiFe single layer as a function of magnetic layer thickness [24].

Table 1. Various antiferromagnets for spin-valve read heads in HDD

		Material system		Crystalline structure	Blocking temp.
Metals	Disordered Alloys	γ-Mn Sys.	Ir-Mn Rh-Mn Ru-Mn	f.c.c.	$\sim 250°C$
		Fe-Mn Sys.	Fe-Mn		$\sim 150°C$
		Cr-Mn Sys.	Cr-Mn-Pt	b.c.c.	$\sim 350°C$
	Ordered Alloys	NiMn Sys.	NiMn PdNiMn PtMn	f.c.t.	$\sim 400°C$
	Oxides	NiO Sys.	NiO	NaCl	$\sim 200°C$
		α-Fe_2O_3 Sys.	α-Fe_2O_3	Al_2O_3	

potential barrier height and width, respectively. Thus, the tunneling probability is higher for the parallel magnetizations than the antiparallel magnetizations in Fig. 10. Equation (4) leads to the magnitude of the TMR at a small bias voltage given by

$$\mathrm{TMR} = (R_{\mathrm{AF}} - R_{\mathrm{F}})/R_{\mathrm{F}} = 2P_1P_2/(1 - P_1P_2) \qquad (6)$$

where R_{AF} and R_{F} are resistance of antiparallel and parallel ferromagnetic spin configurations, respectively and $P_i(i = 1, 2) = [D_{i\uparrow}(E_{\mathrm{F}}) - D_{i\downarrow}(E_{\mathrm{F}})]/[D_{i\uparrow}(E_{\mathrm{F}}) + D_{i\downarrow}(E_{\mathrm{F}})]$ is the spin polarization of the FM electrodes.

Recently, large magnetoresistance up to 20–25% has been observed at *RT* in the ferromagnetic tunnel junctions such as FM-Al_2O_3-FM' with FM and FM' = Fe, Co and NiFe [15–18]. The TMR and related M-H curves at *RT* are shown for Fe/Al_2O_3/Fe junction, as an example, in Fig. 11 [15]. Spinvalve like tunnel junctions have also been developed, in which one of the ferromagnetic layers is pinned by the adjacent antiferromagnetic layer [17,18]. This structure can lead to antiferromagnetic arrangement of the two ferromagnetic layers more easily than the conventional type, results in higher TMR. Ferromagnetic tunnel junctions have large field sensitivity (over 5%/Oe) due to the negligible interlayer coupling, thus technological advantages over spin-valve type GMR may be expected.

5. GMR Heads

One of the most important magnetic field sensors is magnetic read heads for high density magnetic recording. Figure 12 illustrates the historical trend

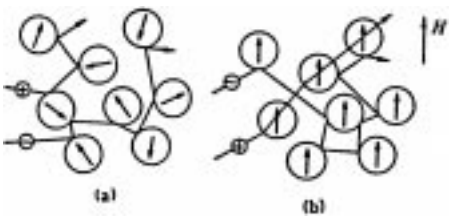

Fig. 9. Spin dependent scattering in metallic granular films.

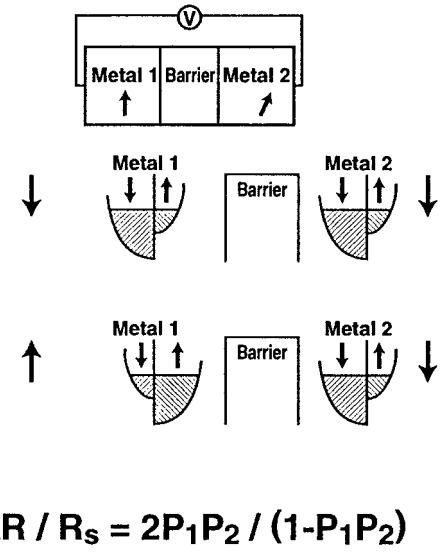

Fig. 10. A schematic model for spin dependent tunneling.

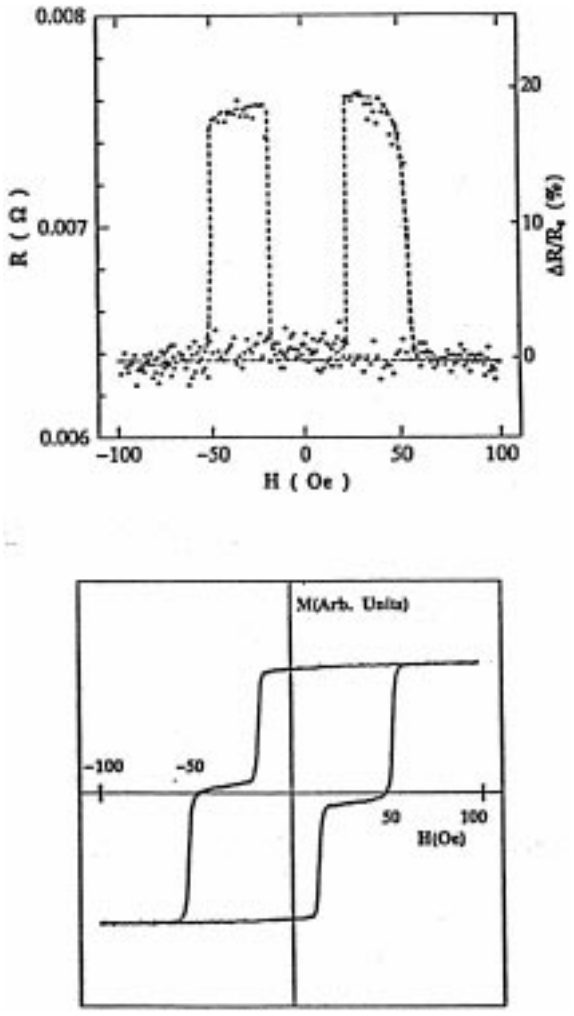

Fig. 11. Magnetoresistance as a function of magnetic field (a) and corresponding hysteresis curve in an 100 nm Fe/Al_2O_3/100 nm Fe tunnel junction [15].

of areal recording density in hard disk drives (HDD). The change in slope in 1990 can be ascribed to a number of important factors, including the shift to smaller disk diameters (which allows more rapid design and integration), the use of thin film disks and advanced heads that possess intrinsic signal-to-noise advantages over earlier types, improvements in design productivity for disk drive electronics and attachment methods. In particular, the use of MR heads using permalloy AMR materials in place of the inductive heads is one of the key factors for the slope change.

The spin-valve GMR is expected to be used in read heads for ultra high density magnetic recording in the next generation because of the high field sensitivity compared to AMR heads. In spin-valve read heads, the spins of the pinned and the free layers are oriented of 90° to each other in order that the spins in the free layer can rotate without hysteresis as shown in Fig. 13. The magnetic moment of the pinned layer is typically fixed along the transverse direction by exchange coupling with an antiferromagnetic layer, while the magnetic moment of the free layer is allowed to rotate in response to signal fields. The resultant spin-valve response is given by

$$\begin{aligned}\Delta R &\propto (\Delta R/R)(R_s W/h)\cos(\theta_1 - \theta_2)\\ &\propto (\Delta R/R)(R_s W/h)\sin\theta_1 \end{aligned} \tag{7}$$

where θ_1 and $\theta_2 (= \pi/2)$ represent the directions of free and pinned layer magnetic moments, respectively, W and h are track width and height of the GMR head, respectively. If the uniaxial anisotropy hard-axis of the free layer is oriented along the transverse signal field direction, then the magnetic signal response is linear ($\sin\theta_1 \propto H$), yielding in turn a linear spin-valve sensor response through Eq. (7).

Figure 14 illustrates reading principle using a GMR head. When a media is moved from left to right the magnetization direction of the free layer of the GMR film changes according to the magnetization direction of the media, which induces resistance change in the GMR head. If we measure the voltage between the two electrodes by applying a current, we can detect the resistance change as a voltage change. The spin valve GMR read heads have been developed for 5 Gb/in^2 [26,27] and 8 Gb/in^2 [28] density recordings. Figure 15 shows the GMR head for 5 Gb/in^2 with a 1 μm track width [27], in which $Co_{90}Fe_{10}$/NiFe/amorphous CoZrNb and $Co_{90}Fe_{10}$ were used for free and pinned layers, respectively. The IrMn was used as an antiferromagnet for exchange biasing, and CoPt hard magnets were used for controlling the magnetic domain structure of the free layer. The read-back voltage waveform obtained by using the GMR head is shown in Fig. 16, which exhibits 1300 μ V_{pp}/μm track. This value is about 3 times higher than that of AMR heads.

6. Future Directions

The trend in Fig. 12 gives an expectation of 10 and 40 Gb/in^2 areal recording densities in 2000 and 2003,

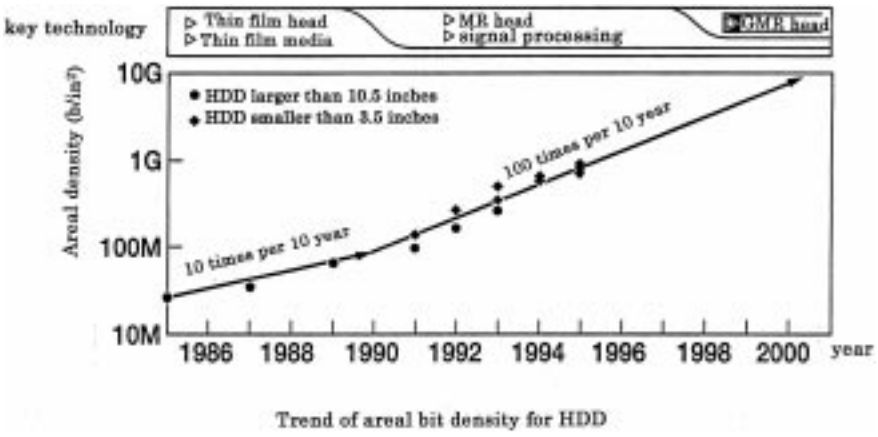

Fig. 12. Historical trend of areal recording density in hard disk drives.

respectively. The spin valve GMR heads are one of the key technologies for the realization. The new read heads with higher field sensitivity, however, may be required for the higher areal density than 40 Gb/in^2. Ferromagnetic tunnel junctions are one of the most promising candidates, because they have high field sensitivity and a simple structure, and submicron size is possible with high junction resistance and low-power dissipation. Even higher field sensitivity is to be expected for the ferromagnetic tunnel junctions with higher spin polarization materials such as half metallic ferromagnets AMnSb with $A =$ Ni and Pt and doped perovskite manganates $R_{1-x}B_xMnO_3$ with $R =$ rare-earth element and $B =$ alkaline earth element

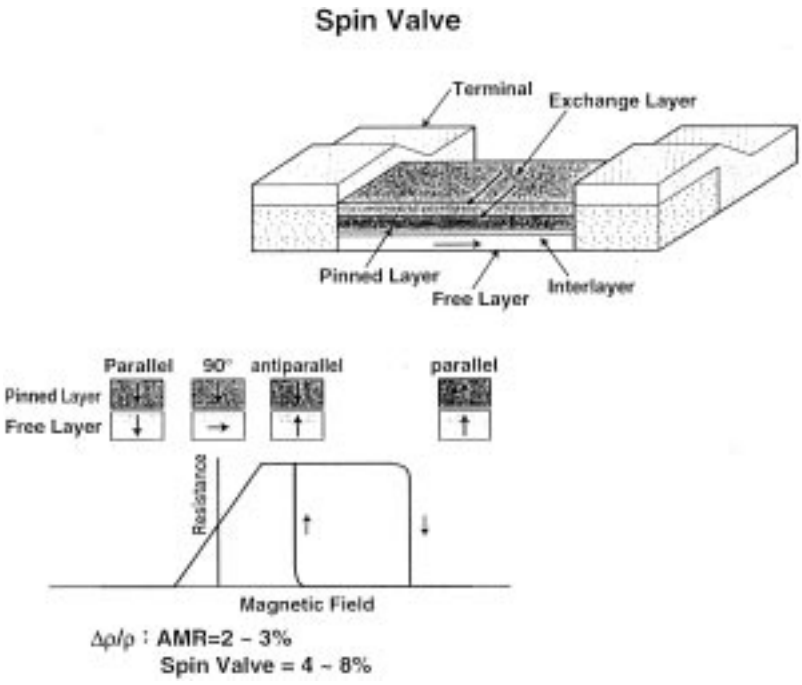

Fig. 13. A schematic spin-valve read head structure and the resistance change vs. applied field.

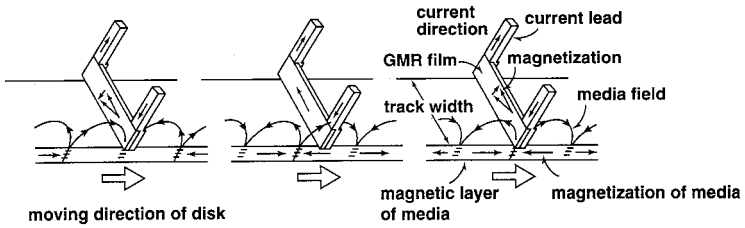

Fig. 14. Reading principle using a GMR head.

[29,30]. The success of ferromagnetic tunneling, however, depends critically on the quality of the insulating tunnel barrier in a trilayer structure. Tunneling is extremely surface sensitive, in that it displays the band structure of the electrodes' surface very close to the barrier insulator. Thus, a good interface and a clean insulator are required for high values of the TMR, which is very challenging. Furthermore, the impedance of tunnel junctions reaches several MΩ, when the junction area is decreased to a few square microns for device applications, inducing noise problems. Thus, ferromagnetic tunnel junctions with a low impedance must be provided for the sensor applications. Recently, a ferromagnetic tunnel junction with novel structure was proposed for meeting the requirement, in which a nano-structured ferromagnetic granular film is sandwiched between two soft ferromagnetic layers [31]. The nano-structured granular film consists of layered nano-sized hard magnetic metallic particles embedded in an insulating matrix.

After the discovery of GMR, a new field called ''spin electronics'' is growing dramatically, in which spin polarized transports such as spin-dependent scattering and spin-dependent tunneling in magnetic thin films are utilized. Three terminal devices such as bipolar spin-transistors [32] and spin-valve transistors [33] have been provided. The former is a ferromagnetic-nonmagnetic-ferromagnetic trilayer three-terminal device fabricated solely from metal films with a bipolar voltage (or current) output that depends on the orientation of the magnetizations of two ferromagnetic layers. The latter consists of a ferromagnetic multilayer sandwiched between two potential barriers. The emitter barrier injects hot electrons into the spin-valve base, the collector barrier accepts only ballistic electrons, making the collector current very sensitive to magnetic fields. Room temperature operation has been accomplished by preparing Si-Co-Cu-Co-Si devices by vaccum metal bonding [34].

The GMR has provided us with a new viewpoint both for understanding the electronic properties of solids and for exploiting these properties to generate new effects. These effects will soon be the basis for electronic devices in the new field of spin electronics.

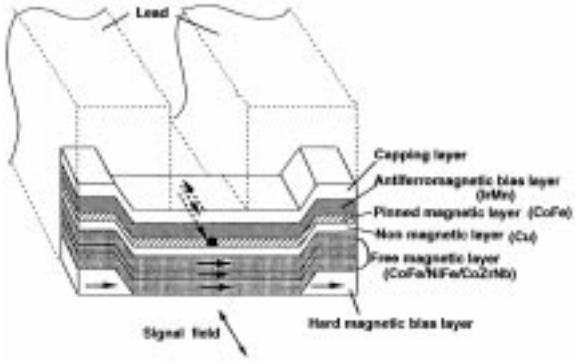

Fig. 15. A GMR read head for 5 Gb/in^2 with 1 μm track width [27].

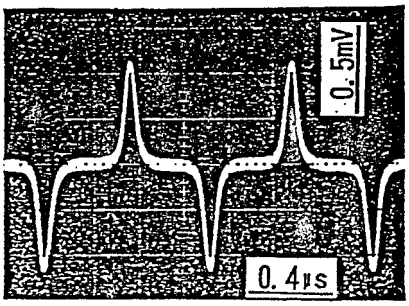

Fig. 16. Read-back voltage waveform obtained by the GMR head in Fig. 15, exhibiting 1300 μ V/μm track [27].

References

1. M.N. Baibich, J.B. Broto, A. Fert, F.N. Van Dau, F. Petroff, P. Etienne, G. Creuset, A. Friedrich, and J. Chazelas, *Phys. Rev. Lett.*, **61**, 2472 (1988).
2. S.S.P. Parkin, R. Bhadra, and K.P. Roche, *Phys. Rev. Lett.*, **66**, 2152 (1991).
3. D.H. Mosca, F. Petroff, A. Fert, P.A. Schroder, W.P. Pratt Jr, and R. Laloee, *J. Magn. Magn. Mater.*, **94**, L1 (1991).
4. T. Shinjo and H. Yamamoto, *J. Phys. Soc. Jpn.*, **59**, 3061 (1990).
5. J.Q. Xiao, J. Samuel, and C.L. Chien, *Phys. Rev. Lett.*, **68**, 3749 (1992).
6. A.E. Berkowitz, J.R. Mitchell, M.J. Corey, A.P. Young, S. Zhang, F.E. Spada, F.T. Parker, A. Hatton, and G. Thomas, *Phys. Rev. Lett.*, **68**, 3745 (1992).
7. B. Dieny, V.S. Speriosu, S.S.P. Parkin, B.A. Gurney, D.R. Wilhoit, and D. Mauri, *Phys. Rev.*, **B43**, 1297 (1991).
8. C. Tsang et al., *IEEE Trans., Mag.*, **30**, 3801 (1994).
9. H. Kanai et al., *IEEE Trans. Mag.*, **31**, 2612 (1995).
10. A.V. Pohm, R.S. Beech, J.M. Daughton, B.A. Everitt, E.Y. Chen, M. Durlan, K. Nordquist, T. Zhu, and S. Tehrani, *IEEE Trans. Mag.*, **32**, 4645 (1996).
11. D.D. Tsang et al., *IEEE Trans. Mag.*, **31**, 3206 (1995).
12. J.L. Brown and A.V. Pohm, *IEEE Trans. Mag.*, **17**, 373 (1994).
13. M. Julliere, *Phys. Lett.*, **54A**, 225 (1975).
14. H. Fujimori et al., *Mat. Sci. Eng.*, **B31**, 219 (1995).
15. T. Miyazaki and N. Tezuka, *J. Magn. Magn. Mater.*, **139**, L231 (1995).
16. J.S. Moodera, L.R. Kinder, T.M. Wong, and R. Moservey, *Phys. Rev. Lett.*, **74**, 3273 (1995).
17. M. Sato and K. Kobayashi, *Jpn. J. Appl. Phys.*, **36**, L200 (1997).
18. W.J. Gallagher et al., *J. Appl. Phys.*, **81**, 3741 (1997).
19. Y. Saito and K. Inomata, *Jpn. J. Appl. Phys.*, **30**, L1733 (1991).
20. K. Inomata and Y. Saito, *J. Magn. Magn. Mater.*, **126**, 425 (1993).
21. H. Kubota and T. Miyazaki, *J. Magn. Soc. Jpn.*, **18**, 335 (1994).
22. R.L. White, *IEEE Trans. Mag.*, **28**, 2482 (1992).
23. J. Inoue, A. Oguri, and S. Maekawa, *J. Phys. Soc. Jpn.*, **60**, 376 (1991).
24. Y. Kamiguchi et al., *J. Magn. Soc. Jpn.*, **18**, 341 (1994).
25. Maekawa and U. Gafvert, *IEEE Trans. Mag.*, **18**, 707 (1982).
26. H. Mutoh, H. Kanai, I. Okamoto, Y. Ohtsuka, T. Sugawara, J. Koshikawa, J. Yoda, Y. Uematsu, M. Shinohara, and Y. Mizoshita, *IEEE Trans. Mag.*, **32**, 3914 (1996).
27. H. Yoda, A. Hori, N. Inoue, A. Sawabe, and M. Sahashi, *IEEE Trns. Mag.*, **31**, 2666 (1995).
28. H. Kanai, J. Kane, K. Yamada, K. Aoshima, J. Toda, and Y. Mizoshita, *IEEE Trans. Mag.*, **33**, 2872 (1997).
29. M. Viret et al., *Europhys. Lett.*, **39**, 545 (1997).
30. J.Z. Sun et al., *Appl. Phys. Lett.*, **69**, 3266 (1996).
31. K. Inomata et al., *Jpn. J. Appl. Phys.*, **36**, L1380 (1997).
32. M. Johnson, *Science*, **260**, 320 (1993).
33. D.J. Monsma et al., *Phys. Rev. Lett.*, **74**, 5200 (1995).
34. D.J. Monsma et al., *Science*, to be published.